

Investigation of the $\Delta I = 2$ Staggering in the Superdeformed Bands of ^{194}Hg Nuclei

K. A. Gado^{a,b}

^a Department of Physics, Faculty of Science, Al-Baha University, Saudi Arabia.

^b Basic Sciences Department, Bilbeis Higher Institute for Engineering (BHIE), Bilbeis 44713, Sharqia, Egypt.

Doi: <https://doi.org/10.47011/18.2.7>

Received on: 15/11/2023;

Accepted on: 13/03/2024

Abstract: The bandhead spin I_0 was determined by solving a quadratic equation based on the Harris parameters, α, β, γ , and δ , which were obtained by fitting the experimental dynamical moment of inertia ϑ_2 to the experimental rotational frequency ω . Due to its high compatibility with the gamma transition energies, the four-parameter collective rotational model of Bohr-Mottelson was employed to predict the transition energies and spins of the levels in the superdeformed (SD) bands of ^{194}Hg (b_1, b_2, b_3). The results show that the energy spectra obtained from the four-parameter collective rotational model are more accurate than those obtained previously. For the $A \sim 190$ mass region, ϑ_2 increases with increasing ω . It is suggested that a discrete approximation of the fourth derivative of the energy difference as a function of angular momentum can appropriately define the staggering in the bands for ^{194}Hg (b_1, b_2, b_3) superdeformed (SD) nuclei. In ^{194}Hg (b_1, b_2, b_3) with long bands ($I \geq 9$), this quantity displays a well-developed staggering pattern (zigzagging behaviour with alternating signs). The interaction between two sequences is shown to account for the staggering in a reasonable way. The model energy expression reproduces successfully the staggering pattern in all considered SD bands for ^{194}Hg (b_1, b_2, b_3) up to $I \sim 50$.

Keywords: Superdeformed band, Spin assignment, Bohr-Mottelson model.

Introduction

In the mass ranges $A \sim 190, 150, 130, 80$, and 60, many SD bands have been found since the discovery of an SD rotational band in the rapidly spinning nucleus ^{152}Dy [1]. Sadly, gamma energies are the sole publicly available spectroscopic data for the SD bands, as discrete linking transitions between the low-lying normal deformation (ND) states and the SD states have not been observed [2]. The sole method to determine the spin value is theoretical, as there is little experimental data available for the spin of the rotational bands. There are several methods that have been suggested for giving spins to SD states [3]. These methods include both direct and indirect ways to give the states in the SD bands a spin. The direct method expresses the energy of

the states of a rotating band as a function of spin, as demonstrated in our earlier studies [4, 5]. Conversely, the indirect methods primarily depend on the use of the Harris formula to match the experimental dynamical moment of inertia data [6]. The spin is then computed using the parameters derived from the fit. The spin can be described as an expansion in the rotational frequency in such a parameterization. Since SD states were seen down to relatively low spin and most bands have very similar, gradually rising dynamical moment of inertia values as increasing rotational frequency, the SD bands in the $A \sim 190$ region are of great interest. The gradual alignment of high-j intruder protons and neutrons in pairs, together with pair correlations,

is the common source of this smooth rise in the dynamical moment of inertia. The $i_{13}^{\frac{1}{2}}$ protons and $j_{15}^{\frac{1}{2}}$ neutrons are the intruder orbitals that cause band crossing. Throughout the $A \sim 190$ region, there is virtually no variation in the high- N intruder orbital structure [7]. As a function of spin or rotational frequency, some SD nuclear bands exhibit a zigzag behavior in gamma transition energies. This is referred to as bifurcation or $\Delta I = 2$ staggering. Two $\Delta I = 4$ sequences with spin values $I + 4n$ and $I + 4n + 2$ ($n = 0, 1, 2, 3, \dots$) are formed when the bands were perturbed. There are several interpretations for the $\Delta I = 2$ energy staggering. In contrast to a 180° rotation, which yields a typical $\Delta I = 2$ sequence, Hamamoto and Mottelson [8] proposed that there may be evidence for a novel symmetry in the nuclear Hamiltonian, specifically, invariance under a 90° rotation about a rotational axis. According to Pavlichenkov and Flibotte [9], the alignment of total nuclear angular momentum along the axis perpendicular to the long deformation axis of a prolate nucleus is thought to be connected to the staggering. According to Macchiavelli *et al.* [10], the $\Delta I = 2$ staggering results from the mixing of many rotating bands with $\Delta I = 4$ differences. The purpose of this study is to discuss the genesis of $\Delta I = 2$ staggering in the $A \sim 190$ mass region and to highlight several theoretical characteristics that are utilized to characterize the properties of SD nuclei. Specifically, we provide a way to assign bandhead spin. More than 85 SD bands have been detected in the $A = 190$ mass range alone in Au, Hg, Tl, Pb, Bi, and Po nuclei, making it a region of particular interest.

2. Bohr-Mottelson Model: Mathematical Review

In Ref. [11], the rotational energy is described as a function of $I(I + 1)$. An extension in powers of $I(I + 1)$ can be used for small enough values of I .

$$E_{rot}[I(I + 1)] = AI(I + 1) + B[I(I + 1)]^2 + C[I(I + 1)]^3 + D[I(I + 1)]^4 + \dots \quad (1)$$

Here, B, C, D, \dots are corresponding higher-order inertial parameters, and A is the intrinsic matrix element. The ratio of angular momentum, $\hat{I} = \sqrt{I(I + 1)}$, to angular frequency, ω , is known as the kinematic moment of inertia, ϑ_1 .

$$\vartheta_1 = \frac{\hbar I}{\omega}. \quad (2)$$

But

$$\omega = \frac{1}{\hbar} \frac{dE}{dI}. \quad (3)$$

Substituting Eq. (3) into Eq. (2), we get:

$$\vartheta_1 = \frac{\hbar^2}{2} \left[\frac{dE}{dI^2} \right]^{-1}. \quad (4)$$

One can easily demonstrate from the set of Eqs. (2)-(4):

$$\frac{dE}{d\omega^2} = \frac{dE}{dI^2} \frac{dI^2}{d\omega^2} = \frac{\hbar^2}{2\vartheta_1} \frac{d(\omega^2 \vartheta_1^2)}{\hbar^2 d\omega^2} = \frac{1}{2\vartheta_1} \left[\vartheta_1^2 + 2\vartheta_1 \omega^2 \frac{d\vartheta_1}{d\omega^2} \right] = \frac{1}{2} \vartheta_1 + \omega^2 \frac{d\vartheta_1}{d\omega^2}. \quad (5)$$

Differentiating Eq. (1) with respect to \hat{I}^2 and using the expansion $(1 + x)^{-1}$ with $x = 2 \frac{B}{A} \hat{I}^2 + 3 \frac{C}{A} \hat{I}^4$, and neglecting higher-order terms due to their negligible influence at high spins, we find:

$$\vartheta_1 = \frac{\hbar^2}{2} \frac{1}{A} - \hbar^2 \frac{B}{A^2} \hat{I}^2 + \frac{\hbar^2}{2} \left(\frac{4B^2}{A^3} - \frac{3C}{A^2} \right) \hat{I}^4 + 6\hbar^2 \frac{BC}{A^3} \hat{I}^6 \quad (6)$$

An alternative approach substitutes the square of the angular velocity ω^2 as the expansion parameter in lieu of the variable \hat{I}^2 .

$$\vartheta_1 = \frac{\hbar^2}{2} \frac{1}{A} - \hbar^2 \frac{B}{A^2} \omega^2 + \frac{\hbar^2}{2} \left(\frac{4B^2}{A^3} - \frac{3C}{A^2} \right) \omega^4 + 6\hbar^2 \frac{BC}{A^3} \omega^6 \quad (7)$$

Introducing Harris parameters, α, β, γ , and δ , the above equation reads [12]:

$$\vartheta_1 = \alpha - \beta \omega^2 + \gamma \omega^4 + \delta \omega^6 \quad (8)$$

Substitute the following for Eq. (5):

$$E(\omega) = \frac{1}{2} \alpha \omega^2 + \frac{3}{4} \beta \omega^4 + \frac{5}{6} \gamma \omega^6 + \frac{7}{8} \delta \omega^8. \quad (9)$$

From Eq. (3), one may find the dynamical moment of inertia by:

$$\begin{aligned} \omega \hbar d\hat{I} &= dE \\ \omega \hbar \frac{d\hat{I}}{d\omega} &= \frac{dE}{d\omega} \\ \vartheta_2 &= \frac{1}{\omega} \frac{dE}{d\omega}. \end{aligned} \quad (10)$$

Substitute the following for Eq. (9). After some simplification, we get:

$$\vartheta_2(\omega) = \alpha + 3\beta \omega^2 + 5\gamma \omega^4 + 7\delta \omega^6. \quad (11)$$

By fitting the experimental dynamical moment of inertia, defined as: $\vartheta_2 = \frac{4\hbar^2}{\Delta E_\gamma(I)}$

where $\Delta E_\gamma(I) = E_\gamma(I+2) - E_\gamma(I)$, and the experimental rotational frequency $\hbar\omega(I) = \frac{E_\gamma(I+2) + E_\gamma(I)}{4}$ one can extract the parameters α, β, γ and δ . As mentioned in the introduction, the relationship $\vartheta_2 = \hbar \frac{dI}{d\omega}$ may be used to indirectly determine the band head spin by integrating Eq. (11) with respect to ω , leading to an expression for intermediate spin:

$$\hbar I = \alpha\omega + \beta\omega^3 + \gamma\omega^5 + \delta\omega^7 + c, \quad (12)$$

where c is the constant of integration. Leave this to C. L. Wu [13]. For SD band cascade:

$$I_0 + 2n \rightarrow I_0 + 2n - 2 \rightarrow \dots \rightarrow I_0 + 2 \rightarrow I_0. \quad (13)$$

The transition energies that were noticed are: $E_\gamma(I_0 + 2n), E_\gamma(I_0 + 2n - 2), E_\gamma(I_0 + 2n - 4), \dots, E_\gamma(I_0 + 4), E_\gamma(I_0 + 2)$, where I_0 is the bandhead spin. As long as the discriminant is greater than or equal to zero, the bandhead spin may be determined using Eq. (12), as follows:

$$I_0^2 + 5I_0 + 6 - (\alpha\omega + \beta\omega^3 + \gamma\omega^5 + \delta\omega^7)^2 = 0. \quad (14)$$

The bandhead spin, I_0 , is rounded to the nearest integer and is regarded as a free parameter. One way to confirm the effectiveness of the four-parameter collective rotational model

for the Bohr-Mottelson is to observe the fluctuation in the experimental transition energies $E_\gamma(I)$ for ^{194}Hg (b_1, b_2, b_3) in a SD band ($\Delta I = 2$ staggering effect). In order to examine the $\Delta I = 2$ staggering in further detail, one computes the fourth derivative of the transition energies $\Delta^4 E_\gamma(I)$ at a given spin I by [14]:

$$\Delta^4 E_\gamma(I) = 2^{-4} [E_\gamma(I+4) - 4E_\gamma(I+2) + 6E_\gamma(I) - 4E_\gamma(I-2) + E_\gamma(I-4)]. \quad (15)$$

To be able to track higher-order changes in the SD bands' transition energies, we decided to employ the equation above.

3. Results and Discussion

We calculated I_0 of the SD bands of ^{194}Hg (b_1, b_2, b_3) using the Harris expansion for the current situation where we only know the experimental transition energies. The experimental dynamical moment of inertia was firstly fitted with rotational frequency using Eq. (11), and the band-head spin of the SD bands of ^{194}Hg (b_1, b_2, b_3) was then obtained by solving the quadratic Eq. (14), using the Harris parameters [15]. These parameter values, obtained from the fitting procedure, are presented in Table 1.

TABLE 1. The optimal Harris parameters were computed and adopted for the chosen SD nuclei in order to examine the bandhead spins.

SD band	Optimal Harris Parameters			
	$\alpha[\hbar^8 \text{MeV}^{-7}] \times 10^1$	$\beta[\hbar^6 \text{MeV}^{-5}] \times 10^1$	$\gamma[\hbar^4 \text{MeV}^{-3}] \times 10^2$	$\delta[\hbar^2 \text{MeV}^{-1}] \times 10^3$
$^{194}\text{Hg}(b_1)$	1.32	2.02	4.53	-2.09
$^{194}\text{Hg}(b_2)$	1.37	1.56	3.29	-1.34
$^{194}\text{Hg}(b_3)$	1.37	2.25	2.07	-0.92

Unfortunately, as indicated by Eq. (12)—specifically the integration constant—such a process involves some uncertainty. In order to resolve this stalemate, as imposed by C. L. Wu

[13], the constant c is considered to be the initial alignment i_0 , which can be assumed to be zero, since no alignment occurs at $\omega = 0$.

TABLE 2. Values of bandhead spin I_0 for studied SD bands, where b_1, b_2 , and b_3 refer to band number 1, band number 2, and band number 3, respectively.

SD band	Bandhead spin, $I_0[\hbar]$			
	Present Work (PW)	Ref. [11]	Ref. [16]	Exp. [17]
$^{194}\text{Hg}(b_1)$	8	8	8	8
$^{194}\text{Hg}(b_2)$	7	8	8	8
$^{194}\text{Hg}(b_3)$	7	9	11	9

Table 2 clearly shows that the bandhead spin of the SD band of the ^{194}Hg (b_1) is in good agreement with both the experimental analysis [17] and the theoretical analyses [11, 16]. In the

second SD band, ^{194}Hg (b_2), the shift of spin levels from even to odd is attributed to a one-unit decrease in the band-head spin. Finally, for the third SD band, $^{194}\text{Hg}(b_3)$, the deviation in band-

head spin compared to Ref. [17] is the same as that reported in Ref. [16].

Under the adiabatic approximation, the transition energy $E_\gamma(I)E_{\gamma(I)}$

$E_\gamma(I)$ —where I is the spin of the state—can be expressed as:

$$E_\gamma(I) = Dg_4 + Cg_3 + Bg_2 + Ag_1, \quad (16)$$

where the four parameters A, B, C , and D are determined by the Bohr-Mottelson model for an axially symmetric nucleus. Here, $g_i = (I^2 + 5I + 6)^i - (I^2 + I)^i$, $i = 1, 2, 3, 4$. Equation (16) was utilized to fit the angular spins of the experimental transition energies for the SD bands of ^{194}Hg (b_1, b_2, b_3) to get the parameters of our model, as shown in Table 3.

TABLE 3. The optimal parameters of the four-parameter collective rotational model for the Bohr-Mottelson were computed and adopted for the chosen SD nuclei.

SD band	Optimal parameters of the four-parameter collective rotational model			
	$D[\text{MeV}] \times 10^{-14}$	$C[\text{MeV}] \times 10^{-10}$	$B[\text{MeV}] \times 10^{-7}$	$A[\text{MeV}] \times 10^{-3}$
$^{194}\text{Hg}(b_1)$	2.70	-1.60	2.03	4.71
$^{194}\text{Hg}(b_2)$	1.80	-1.01	0.75	7.87
$^{194}\text{Hg}(b_3)$	-0.20	0.33	-2.54	5.33

In the SD band $^{194}\text{Hg}(b_1, b_2, b_3)$, the value of B/A is on the order of 10^{-4} , indicating that B/A

decreases as one approaches the configurations for which the deformed shape is more stable.

TABLE 4. The calculated transition energies, E_γ , for our three SD bands in ^{194}Hg , compared to experimental data and other theoretical models.

SD band	Transition Energy, $E_\gamma[\text{MeV}]$							
	Present Work (PW)		Ref. [11]		Ref. [16]		Exp. [17]	
	I	E_γ	I	E_γ	I	E_γ	I	E_γ
$^{194}\text{Hg}(b_1)$	10	0.219	10	0.204	10	0.208	10	0.212
	12	0.258	12	0.246	12	0.250	12	0.254
	14	0.297	14	0.288	14	0.293	14	0.296
	16	0.336	16	0.330	16	0.335	16	0.337
	18	0.375	18	0.370	18	0.376	18	0.377
	20	0.413	20	0.411	20	0.416	20	0.417
	22	0.452	22	0.450	22	0.456	22	0.455
	24	0.49	24	0.489	24	0.494	24	0.492
	26	0.527	26	0.527	26	0.532	26	0.528
	28	0.563	28	0.563	28	0.569	28	0.563
	30	0.598	30	0.599	30	0.604	30	0.597
	32	0.632	32	0.634	32	0.639	32	0.630
	34	0.664	34	0.668	34	0.672	34	0.662
	36	0.695	36	0.701	36	0.703	36	0.693
	38	0.725	38	0.732	38	0.733	38	0.724
	40	0.754	40	0.762	40	0.762	40	0.754
	42	0.782	42	0.790	42	0.789	42	0.784
	44	0.811	44	0.817	44	0.814	44	0.813
	46	0.841	46	0.843	46	0.837	46	0.843
	48	0.874	48	0.867	48	0.858	48	0.872
	50	0.913	50	0.889	50	0.889	50	0.903
$^{194}\text{Hg}(b_2)$	rms	9.05×10^{-3}	1.57×10^{-2}		1.11×10^{-2}			
	9	0.205	10	0.198	10	0.200	10	0.201
	11	0.244	12	0.239	12	0.241	12	0.242
	13	0.283	14	0.280	14	0.282	14	0.283
	15	0.322	16	0.320	16	0.322	16	0.323
	17	0.361	18	0.360	18	0.362	18	0.363
	19	0.400	20	0.400	20	0.402	20	0.402
	21	0.439	22	0.438	22	0.441	22	0.440
	23	0.476	24	0.476	24	0.479	24	0.478

SD band	Transition Energy, $E_\gamma [\text{MeV}]$							
	Present Work (PW)		Ref. [11]		Ref. [16]		Exp. [17]	
	25	0.514	26	0.514	26	0.516	26	0.514
	27	0.550	28	0.550	28	0.552	28	0.550
	29	0.586	30	0.586	30	0.588	30	0.585
	31	0.620	32	0.621	32	0.623	32	0.619
	33	0.653	34	0.655	34	0.656	34	0.652
	35	0.686	36	0.688	36	0.689	36	0.685
	37	0.717	38	0.720	38	0.720	38	0.716
	39	0.747	40	0.751	40	0.750	40	0.747
	41	0.777	42	0.780	42	0.779	42	0.778
	43	0.806	44	0.808	44	0.806	44	0.808
	45	0.837	46	0.835	46	0.832	46	0.837
	47	0.868	48	0.861	48	0.856	48	0.867
rms	5.35×10^{-3}		6.63×10^{-3}		5.00×10^{-3}			
$^{194}\text{Hg}(b_3)$	9	0.221	11	0.218	13	0.222	11	0.222
	11	0.262	13	0.258	15	0.260	13	0.262
	13	0.303	15	0.299	17	0.301	15	0.303
	15	0.343	17	0.339	19	0.341	17	0.343
	17	0.382	19	0.378	21	0.381	19	0.382
	19	0.420	21	0.418	23	0.420	21	0.420
	21	0.458	23	0.456	25	0.458	23	0.458
	23	0.495	25	0.494	27	0.496	25	0.495
	25	0.531	27	0.531	29	0.533	27	0.531
	27	0.566	29	0.567	31	0.569	29	0.566
	29	0.601	31	0.603	33	0.604	31	0.601
	31	0.635	33	0.637	35	0.639	33	0.635
	33	0.668	35	0.671	37	0.672	35	0.668
	35	0.700	37	0.704	39	0.704	37	0.700
	37	0.732	39	0.736	41	0.736	39	0.732
	39	0.763	41	0.766	43	0.766	41	0.763
	41	0.794	43	0.796	45	0.794	43	0.794
	43	0.824	45	0.824	47	0.822	45	0.824
	45	0.854	47	0.851	49	0.848	47	0.854
	47	0.884	49	0.877	51	0.873	49	0.884
rms	1.01×10^{-3}		7.83×10^{-3}		5.73×10^{-3}			

As shown in Table 4 and based on the root mean square (rms) deviation test results [18], the transition energies E_γ computed with our model correspond better with the experimental values than with other models, particularly for $^{194}\text{Hg}(b_1)$. We conclude that this deviation is due to the difference in the way the issue is addressed between our model and other models. The rotational frequency $\hbar\omega$, kinematic ϑ_1 , and dynamic ϑ_2 moments of inertia are now related in the following way:

$$\hbar\omega(I) = 8D\hat{I}^7 + 6C\hat{I}^5 + 4B\hat{I}^3 + 2A\hat{I}. \quad (17)$$

$$\vartheta_1(I) = \frac{\hbar^2}{8D\hat{I}^6 + 6C\hat{I}^4 + 4B\hat{I}^2 + 2A}. \quad (18)$$

$$\vartheta_2(I) = \frac{\hbar^2}{56D\hat{I}^6 + 30C\hat{I}^4 + 12B\hat{I}^2 + 2A}. \quad (19)$$

Figure 1 shows that the behavior of the kinematic and dynamic inertia moments calculated from our model of $^{194}\text{Hg}(b_1, b_2, b_3)$ is in good agreement with the experimental data, with the dynamic moment showing the closest match. It demonstrates how well our model can describe the moment of inertia's behavior in the rotating region $A \sim 190$. We suggest that the fourth derivative of the transition energy differences [Eq. (15)], as a function of angular momentum I , provides a more accurate representation of the observed staggering in the SD bands of $^{194}\text{Hg}(b_1, b_2, b_3)$ than a plot of the moment of inertia parameter versus the angular momentum. The transition energies between levels differing by two units of angular

momentum are experimentally well-determined quantities:

$$\Delta E_\gamma(I_j) = E_\gamma(I_j + 2) - E_\gamma(I_j). \quad (20)$$

We applied Eq. (15) and Eq. (20) to ^{194}Hg (b_1 , b_2 , b_3). Here, I_j is the angular momentum that

our model assigns, $I_j = I_0 + 2j$, $j = 0, 1, 2, 3, \dots$ to the region $A \sim 190$, for which the experimentally reported transition energies are long enough ($I \geq 9$).

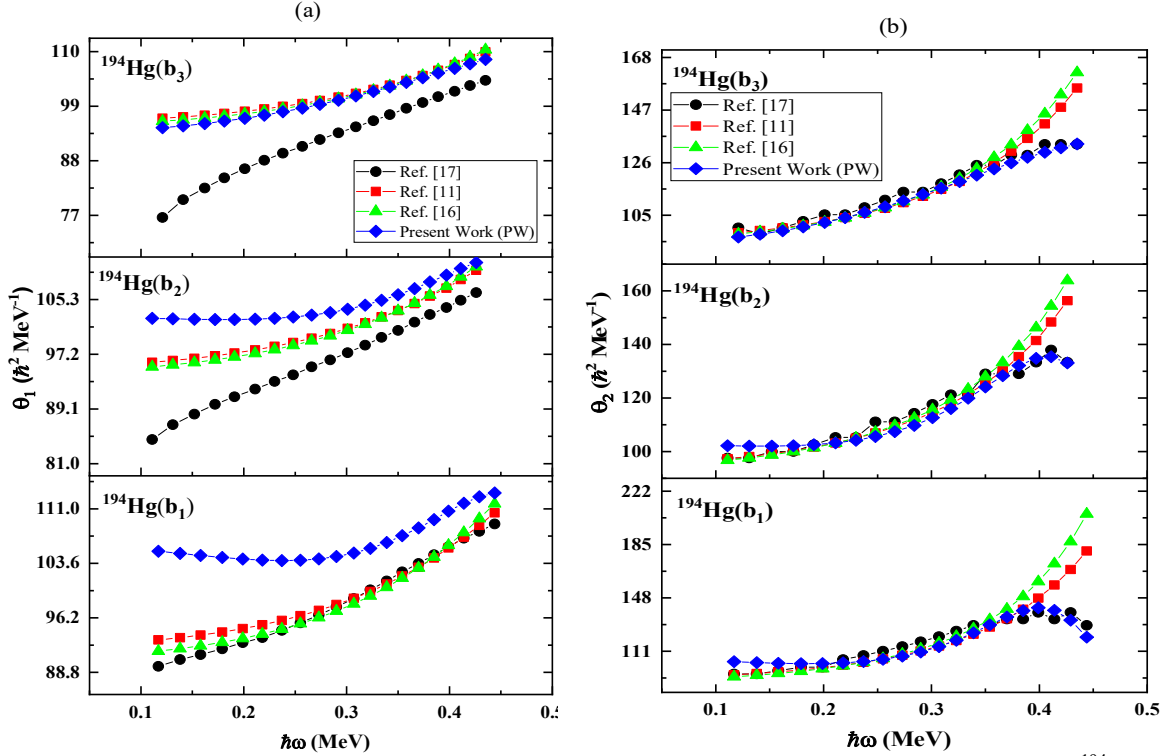


FIG. 1. Predicted (a) kinematic, ϑ_1 , and (b) dynamic, ϑ_2 , moments of inertia for our three SD bands in ^{194}Hg (b_1 , b_2 , b_3) against rotational frequency, $\hbar\omega$, along with a comparison with experimental data and alternative formulae (line with black circles representing, $\Delta^4 E_\gamma^{\text{Cal}}$ resulting from calculated transition energies, line with red squares representing experimental transition energies, and line with blue triangles representing the difference between them).

Figure 2 displays a discernible staggering pattern in all cases, ^{194}Hg (b_1 , b_2 , b_3). Generally, one observes an identical behavior in the staggering between the $\Delta^4 E_\gamma^{\text{Exp}}$ and $\Delta^4 E_\gamma^{\text{Dev}}$ with fluctuations in the amplitude as the angular momentum I increases. This oscillation may be associated with the rotational structure of superdeformed bands of ^{194}Hg (b_1 , b_2 , b_3), which is somewhat perturbed. However, it is reasonable to interpret this behavior of the staggering effect in terms of the interaction between the two sequence bands. The amplitude of the staggering varies only slightly among the different bands.

Therefore, any nonzero values of the parameter $\Delta^4 E_\gamma$ suggest that the order of rotational motion of the nuclear system exceeds \hat{I}^4 . This supports and validates the applicability of our model. The results demonstrate that the four-parameter collective rotational model of Bohr and Mottelson provides a meaningful description of the $\Delta I = 2$ staggering effect in the superdeformed bands of ^{194}Hg (b_1 , b_2 , b_3). Furthermore, the behavior of this effect can potentially be estimated analytically based on collective properties of the nucleus.

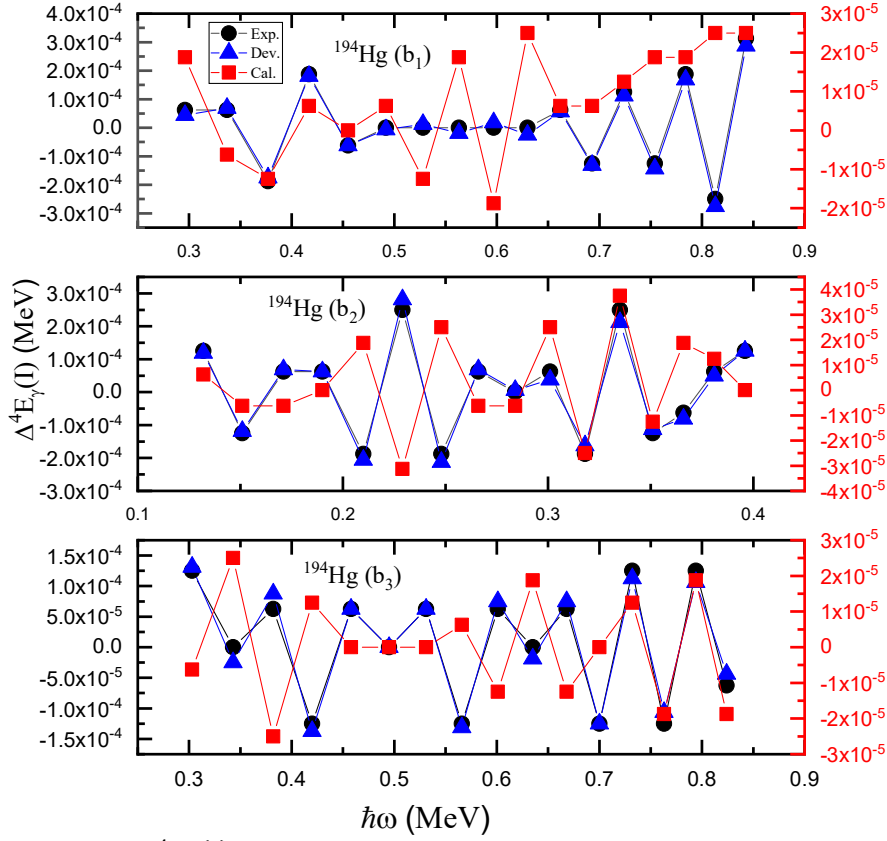


FIG. 2. $\Delta I = 2$ staggering, $\Delta^4 E_\gamma(I)$, calculated using the five-point formula versus nuclear rotational frequency for the SD bands in ^{194}Hg (b_1 , b_2 , b_3), experimental values, and the differences between them.

4. Conclusion

A theoretical version of the Harris four-parameter formula in even powers of angular frequency was used to fit the smoothed experimental dynamical moment of inertia data. A fitting approach was used to modify the expansion parameters. By integrating the computed ϑ_2 , the spins of the SD rotational bands in ^{194}Hg (b_1 , b_2 , b_3) were assigned using the best expansion parameters from the fit by solving the quadratic equation. The closest integer of the fitted I_0 was used to determine the bandhead spin. The values of the bandhead spins of our selected SD band in ^{194}Hg (b_1 , b_2 , b_3) are fairly consistent with all the spin assignments of

other approaches. In the $A \sim 190$ mass region, the dynamical moment of inertia increases with increasing rotational frequency. Within the scope of the four-parameter model, the SD band structure of ^{194}Hg (b_1 , b_2 , b_3) is accurately recreated. The finite difference approximation to the fourth derivative of the gamma transition energies is represented by a smooth reference, which also explains the $\Delta I = 2$ energy staggering found in three of our chosen SD bands. As spin or rotational frequency increases, the parameter $\Delta^4 E_\gamma(I)$ alternates in sign, a behavior characteristic of $\Delta I = 2$ staggering.

References:

- [1] Shalaby, A.S., Commun. Theor. Phys., 41 (3), (2004) 454.
- [2] Shalaby, A.S., Acta Phys. Hung. A, 25 (1) (2006) 117.
- [3] Khalaf, A.M. et al., UPB Sci. Bull., Ser. A, 82 (3) (2020) 231.
- [4] Gado, K.A., Nucl. Phys. At. Energy, 24 (2023) 336.
- [5] Gado, K.A., Nucl. Phys. At. Energy, 25 (1) (2024) 19.
- [6] Khalaf, A.M., Zaki, A.A., and Ismail, A.M., Int. J. Adv. Res. Phys. Sci., 3 (9) (2016) 21.

- [7] Abdalaty, A.A., Kotb, M., Okasha, M.D., and Khalaf, A.M., Phys. At. Nucl., 83 (6) (2020) 849.
- [8] Hamamoto, I. and Mottelson, B., Phys. Lett. B, 333 (1994) 294.
- [9] Pavlichenkov, I.M. and Flibotte, S., Phys. Rev. C, 51 (1995) R460.
- [10] Macchiavelli, A.O. et al., Phys. Rev. C, 51 (1) (1995) R1.
- [11] Okasha, M.D., Glob. J. Sci. Front. Res. A Phys. Space Sci., 14 (3) (2014) 26.
- [12] Khalaf, A.M. et al., Int. J. Theor. Appl. Sci., 7 (2) (2015) 33.
- [13] Wu, C.L., Feng, D.H., and Guidry, M.W., Phys. Rev. Lett., 66 (10) (1991) 1377.
- [14] Semple, A.T. et al., Phys. Rev. Lett., 76 (20) (1996) 3671.
- [15] Saethre, O. et al., Nucl. Phys. A, 207 (1973) 486.
- [16] Khalaf, A.M., Okasha, M.D., and Ragheb, E., Aust. J. Basic Appl. Sci., 10 (16) (2016) 192.
- [17] Singh, B., Zywna, R., and Firestone, R.B., Nucl. Data Sheets, 97 (2002) 241.
- [18] Khalaf, A.M. et al., Int. J. Theor. Appl. Sci., 6 (2) (2014) 47.